JOURNAL OF MATERIALS SCIENCE: MATERIALS IN MEDICINE 9 (1998) 191–196

A finite-element model study of occlusal schemes in full-arch implant restoration

A. APICELLA, E. MASI, L. NICOLAIS
Department of Material and Production Engineering, University of Naples, Federico II, Piazzale Tecchio, 80125 Naples, Italy

F. ZARONE, N. DE ROSA, G. VALLETTA
Istituto di Discipline Odontostomatologiche, University of Naples, Federico II, Piazzale Tecchio, 80125 Naples, Italy

A three-dimensional finite-element model of a human mandible is presented, and the stresses and deformations computed for loading states induced by two different gnathologic reconstructions using six and four implants are discussed. Occlusal canine guidance and posterior and anterior group functions on cantilevered and distally supported prostheses have been simulated. The stress distributions generated by the different loading conditions on either the osseointegrated prosthesis or the bone tissue surrounding the implants are described. The analysis of the stress distribution on the working side reveals that the posterior group function undergoes a reduction in stress intensity on the cortical bone surrounding the implants (especially for the distal implant) compared with the anterior group function and canine guidance in both gnathologic reconstructions.

1. Introduction

Bone growth, remodelling and adaptation are all processes which are believed to be partly regulated in some way by the mechanics of the tissue. This phenomenon has been hypothesized to be driven by microscopic damage which stimulates bone adaptation to reconfigure an optimal bone strength (Wollf's law). A significant modification of the bone's local stress distribution is attained after gnathologic reconstruction. The extent and nature of the remodelling process depend on the shape and rigidity of the occlusal scheme. The mandible, in its natural state, does not share the external loads with the rigid implant and the stress distribution attains a physiological value that stimulates bone growth.

The optimization of the occlusal scheme in gnathologic reconstruction has been controversially debated in the last few decades [1–5]. The fitting of implant–prosthetic rehabilitation with the stomatognathic functions is one of the key points to be analysed for satisfactory long-term functional and aesthetic results. The traditional occlusal principles cannot be directly applied to the implant–prosthetic rehabilitation. The use of osseointegrated prostheses requires, then, a basic theoretical review of these principles, owing to the different biomechanical behaviours with respect to the periodontal system.

The occlusal method, used for the technical realization of the fixed prosthetic superstructure, aims to check the intensity and direction of the forces generated at the bone–implant interface. The importance of occlusal scheme in long-term rehabilitation has been reported in the literature [6, 7]; however, collected data on the subject are fragmentary, extracted from anecdotal clinical cases and often based on individual opinions without any scientific support. At the moment, it is not possible to codify an ideal occlusion model, owing to the lack of data which have been scientifically and medically demonstrated. In particular, the biomechanical transfer of the loads is a significant problem in the total edentia, rehabilitated with fixed prosthesis. The estimation of the biomechanical behaviour of the system is complex, because of the great variability of mechanical, anatomic and restoration aspects which are present during the stomatognathic function [8].

The occlusal solutions suggested by the different schools are often in disagreement. According to Branemark *et al.* [9], both canine guidance and group function should be tolerated by the patients treated with fixed prosthesis supported by implants. In a successive study, Jemt *et al.* [10] found that the patients preferred the group function to the canine guidance. On the contrary, Hobo *et al.* [11] suggested that the posterior distribution of the occlusal loads should generate high lateral stresses on the posterior prosthetic elements. These stresses occur during eccentric movements and can be dangerous for the implants and the bony tissue of the support.

The bone–implant interface can bear a high value of vertical forces, which are parallel to the greater axis of the implants. On the contrary, it does not sustain slanting loads, because these can generate bending

moments and a high stress concentration on the peri-implant marginal bone [12].

A balanced occlusion is, therefore, not appropriate for fixed total restorations on implants [13]. In this case a mutually protected occlusion is preferred. It is therefore possible to avoid the occurrence of dangerous extra-axial forces on the distal sections of edentulous arches during eccentric movements [11, 13]. A disclusion of posterior sections allows a uniform stress distribution on the implants located in the anterior side of the arches, thereby avoiding the danger of overloads [13]. Reitz [14] suggested the use of a lingual occlusion in the posterior sections, connected with an anterior unocclused guidance.

The biomechanical relationship between the different occlusal schemes and the loads distribution on the prosthesis (at the bone–implant interface and at the peri-implant tissues) is therefore not well known and has been investigated in only a few cases [11–4].

Within this framework, we developed a three-dimensional finite-element (FE) model of a human mandible and we analysed the stresses and deformations computed for loading states induced by two different gnatologic reconstructions using six and four implants. Occlusal canine guidance, and posterior and anterior group functions on cantilevered and distally supported prostheses have been simulated. This study was principally aimed at analysing the stress distributions generated by the different loading conditions on either the osseointegrated prosthesis or the bone tissue surrounding the implants.

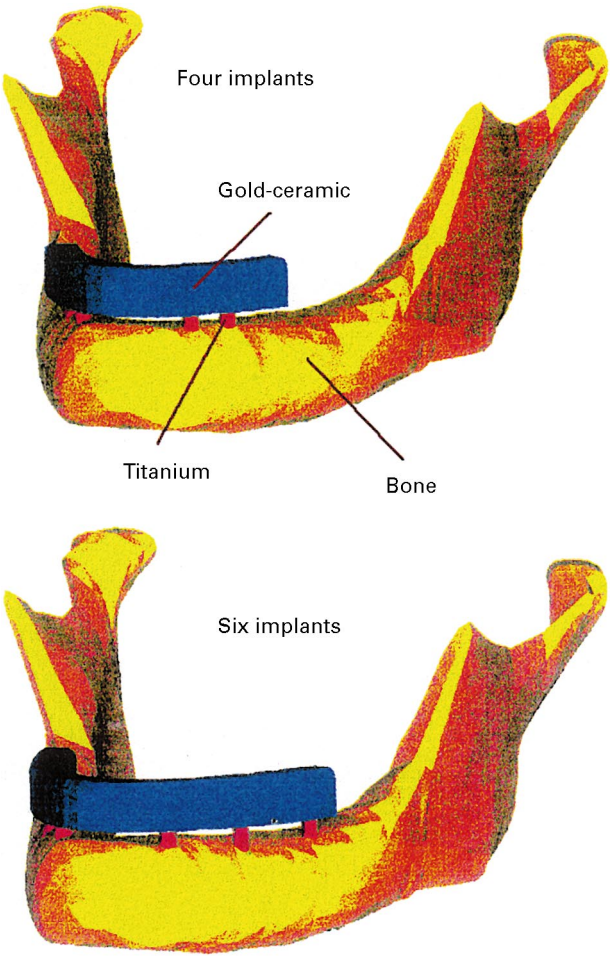

Figure 1 Full-arch bridge and mandible models used in the FE analysis.

2. Materials and methods

The complex geometry of the FE models was constructed according to the following procedure. A human mandible model was imaged in the frontal plane by a laser digitizer. The mandibular section profiles were collected at 3 mm increments. All traces were assembled into a three-dimensional wireframe model by means of an ordinary three-dimensional (3D) CAD (AutoCad 12). Each profile was described by a cubic spline defined by the same number of sections. This procedure allowed us to optimize the construction of the solid model which was obtained by skin groups. The 3D solid and FE models of the mandible and the implants were developed using SDRC I-DEAS VI-i software. The wireframe curve sections were used to define the mesh areas and volumes. The final mandibular FE model was formed by parabolic tetrahedral elements while the full-arch rigid superstructure was designed using linear and parabolic wedge solid elements.

Two 3D solid models of full-arch implant–prosthetic restoration have been realized:

1. a mandible with six implants and a prosthetic superstructure made of a gold–ceramic rod (Fig. 1b);
2. a mandible with four implants and a prosthetic superstructure made of a gold–ceramic bar with distal extensions (Fig 1a).

In both models the implants are placed symmetrically to the midsagittal plane on the two sides of the mandible.

The FE models were restrained from displacements in and rotation around the three principal axes at the condile base and loaded at the anterior and posterior group functions and canine guidance.

After the definition of the FE models, an appropriate choice of materials was made. The bone, the implant and all rigid structure prosthesis materials were considered isotropic.

Moreover, as indicated in Fig. 2 where an implant and the mandible section are shown, the cortical external bone and internal cancellous characteristics of the mandibular bone have been considered in the FE modelling and in the definition of the bone properties. Different mechanical characteristics have been assigned, therefore, to the internal and external model finite elements of the mandible. The material's properties are reported in Table I.

The values of the mechanical properties of the cortical and cancellous bones represent a human mandibular case [15] while those of the rigid titanium alloy and of the ceramic and a gold alloy were taken from the technical literature [16, 17].

3. Results and discussion

In this study we develop a 3D FE analysis, aimed at estimating the deformations and stresses generated by

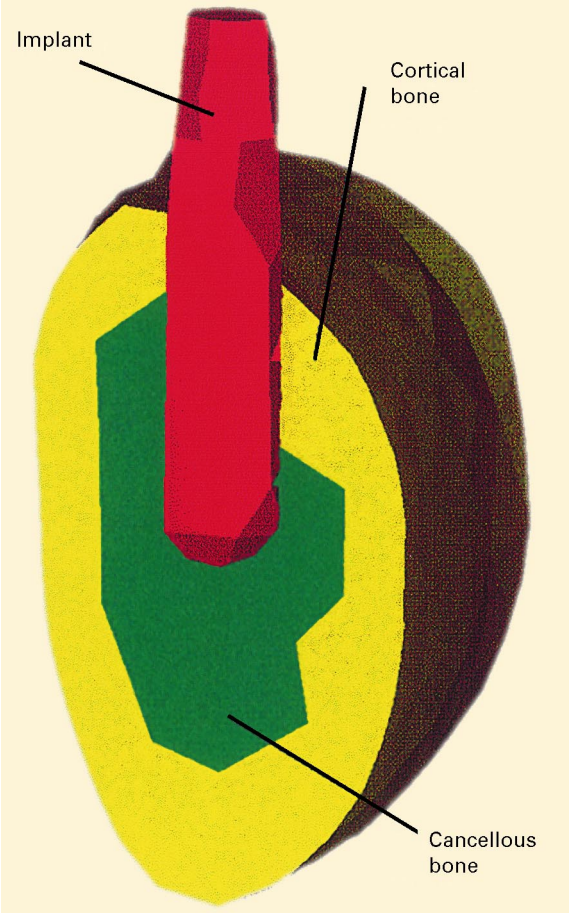

Figure 2 Detail of the implant–bone FE model used in the simulation. Green, cancellous bone; yellow, cortical bone; red, titanium alloy.

TABLE I Mechanical properties of the material used in the FE

Material	*E* (GPa)	Poisson's ratio
Cortical bone	15	0.25
Cancellous bone	1.5	0.29
Titanium alloy	110	0.29
Gold alloy	120	0.25
Ceramic	60	0.29

eccentric loads. The forces have been applied on the prosthetic structure with different occlusal distributions of the load (canine guidance, and posterior group function and anterior group function). They simulate the eccentric forces generated on the prosthetic superstructure, on the implants and the corresponding bone–implant interface.

Three different occlusal schemes have been followed:

1. canine guidance;
2. posterior group function;
3. anterior group function.

An eccentric load of 20 N was applied on the working side (left) in the x–z plane rotated 30° about the x axis. The load was divided into different proportions according to the position of the prosthetic dental elements, which are involved in the load transfer (canine, incisive, pre-molar and molar teeth). The eccentric forces were applied on the left side of the mandible, which was chosen as the working side. The different proportions of the load were determined according to the biomechanical behaviour of the mandible. The latter acts as a 3°-type lever (the muscle power is applied between the fulcrum, i.e., the temporo-mandibular joint, and the resistance, i.e., the dental arches). According to this scheme, therefore, high loads in the distal sections have been applied in the simulation of the anterior and posterior group functions and of the posterior pre-contact [18].

The analysis of 3D models in this study is comparative. It allows us to compare by means of false colours the intensity and distribution of principal stresses in the mandible and around the bone implant for the different restoration situations.

3.1. First model: mandible with six implants

3.1.1. First occlusal scheme: posterior group function

50% of the load was applied to the molar region while the remaining 50% of the load was applied to the pre-molar region, as shown in Fig. 3 where the buccal (B) and lingual (L) prospects of the principal stresses distribution in the mandible are shown.

A uniform distribution of stresses on the implants and at the peri-implant supporting the bone is observed. Stresses are mainly localized on the lingual side of middle and distal implants. The local high stresses are 4.2 MPa and 0.9 MPa in the distal and middle implants, respectively. Stresses in the peri-implant bone reach their highest values on the cortical bone located disto-lingually to the distal implant (1.7 MPa) and on the cortical bone located lingually to the midimplant (0.5 MPa).

By analysing the sections of the mandible at the implant positions, *the stresses in the cancellous and*

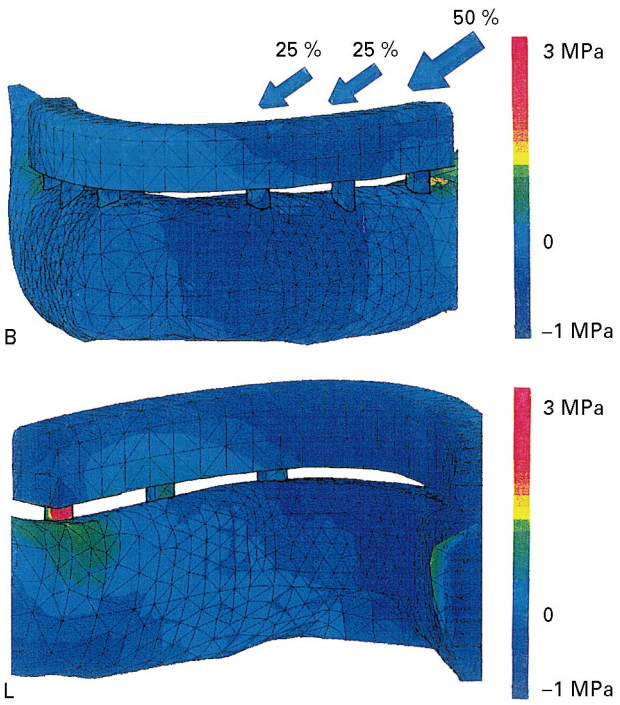

Figure 3 Six-implant model (first occlusal scheme): map of the stress distribution in the posterior group function.

cortical bone surrounding the implants were evaluated. The stresses are evenly distributed in the cortical and cancellous bone surrounding the implant, reaching about 0.2 MPa lingually to the upper part of the bone–distal implant interface for the posterior group function.

3.1.2. Second occlusal scheme: anterior group function and canine guidance

The whole load was applied only to the canine region in the case of canine guidance while it is shared between the central and lateral incisors (55%) and the canine region (45%) in the case of the anterior guidance.

Fig. 4 illustrates the buccal (B) and lingual (L) prospects of the stress distribution in the mandible. These two simulations show similar stresses distributions and hence only the anterior group guidance has been reported. In both cases (concentrated anterior load and distributed load) the maximum principal stresses *on the implants* (5.7–5.8 MPa) are higher than those found in the previous scheme with the posterior group function (4.2 MPa).

The *highest bone stresses* for the antero-occlusal schemes were found disto-lingually to the distal implant spread on the adjacent peri-implant cortical bone. The maximum stress on the peri-implant bone located on the distal implant was 3.0 MPa which, although higher than that evaluated for the posterior group functions (1.7 MPa), is also distributed on a wider cortical bone surface (compare the stress distributions, in the distolingual areas for the first and second occlusal schemes reported in Figs 3 and 4).

In the middle implant, the stresses are concentrated in a small area located lingually to the implant neck; the highest stress in this area is 1.8 MPa for both schemes while they are negligible in the mesial implant. The peri-implant cortical bone is not significantly loaded for the middle and mesial implants.

The *stresses in the cancellous and cortical bone* surrounding the implants were also evaluated. The maximum stresses are concentrated in the apical–lingual portion of the bone–implant interface of the distal implant. The maximum stress value is about 0.7 MPa.

The stress distribution on the working side reveals that the *posterior group function* undergoes a reduction in stress intensity compared with the other occlusal schemes at both the bone–implant interface and the cortical bone surrounding the implants (especially for the distal implant).

3.2. Second model: mandible with four implants with distal extension

3.2.1. First occlusal scheme: posterior group function

50% of the load was applied to the molar region while the remaining 50% of the load was applied to the pre-molar region, as indicated in Fig. 5 where the buccal (B) and lingual (L) prospects of the stress distribution in the mandible are reported.

The highest stress found with this occlusal scheme is 4 MPa (on the lingual surface of implant neck).

In the *peri-implant bone*, the stresses are concentrated mainly on the surface area of the cortical bone located lingually to the implants. In this area the highest stresses are 0.45 MPa (distal implant) and 0.28 MPa (mesial implant).

A section at the distal implant site is reported on the right-hand side of Fig. 7 (posterior group function). The stresses are concentrated in the apical–buccal

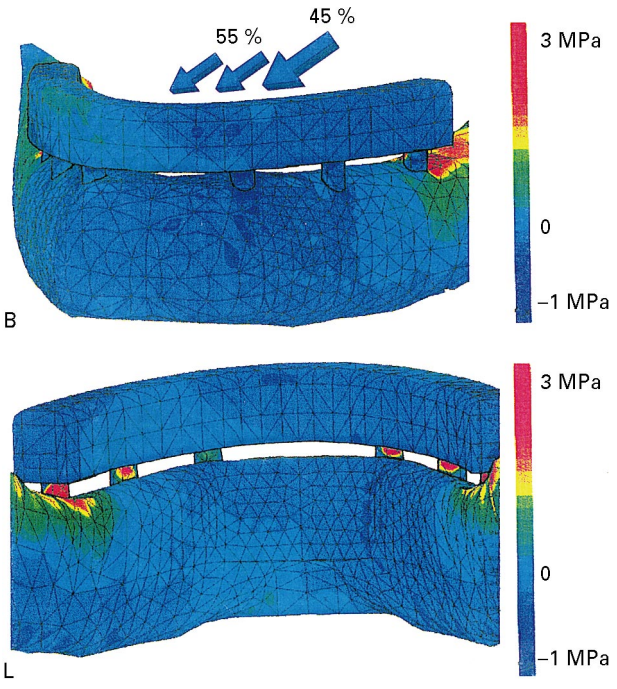

Figure 4 Six-implant model (second occlusal scheme): map of the stress distribution in the anterior group function.

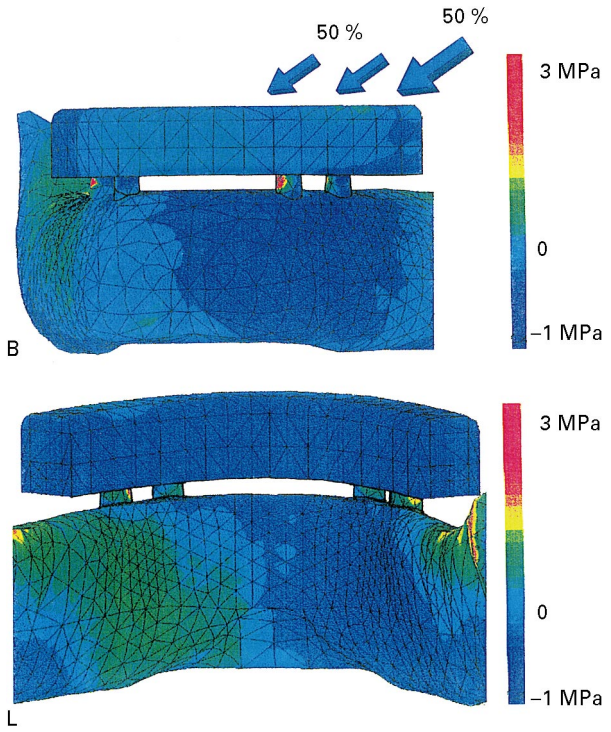

Figure 5 Four-implants model (first occlusal scheme): map of the stress distribution in the posterior group function.

portion of the bone–implant interface. The maximum stress value is about 0.5 MPa.

3.2.2. Second occlusal scheme: anterior group function and canine guidance

The whole load has been applied to the canine region in the case of canine guidance, while for the anterior guidance the load is shared between the central and lateral incisors (55%) and the canine region (45%).

Fig. 7 illustrates the buccal (B) and lingual (L) prospects of the stress distribution in the mandible. As in the first model, the stress distributions in the two schemes are quite similar. Stresses are mainly concentrated on the lingual side of the distal implant on the working side. The maximum stresses detected (5.8 MPa for canine guidance; 6.7 MPa for anterior group function) are higher than those of the posterior group function scheme.

In peri-implant bone the stresses are mainly concentrated on the cortex located lingually to the distal implant. Here, the highest value is 1.6 MPa for the canine guidance and 2.3 MPa for the anterior group function. A section at the distal implant site is reported on the left-hand side of Fig. 6. The stresses are evenly distributed along the bone–implant interface. The maximum stress is about 0.1 MPa.

As in the first model, an analysis of cortical bone stress maps reveals that the posterior group function assures a more uniform distribution in the implants and a reduction in stresses in the peri-implant bone. The analysis of the stresses at the interface between implants and cancellous bone, conversly, showed that in this case the posterior group function induces a higher stress in the implant–bone apical area compared with the anterior group function–canine guidance schemes.

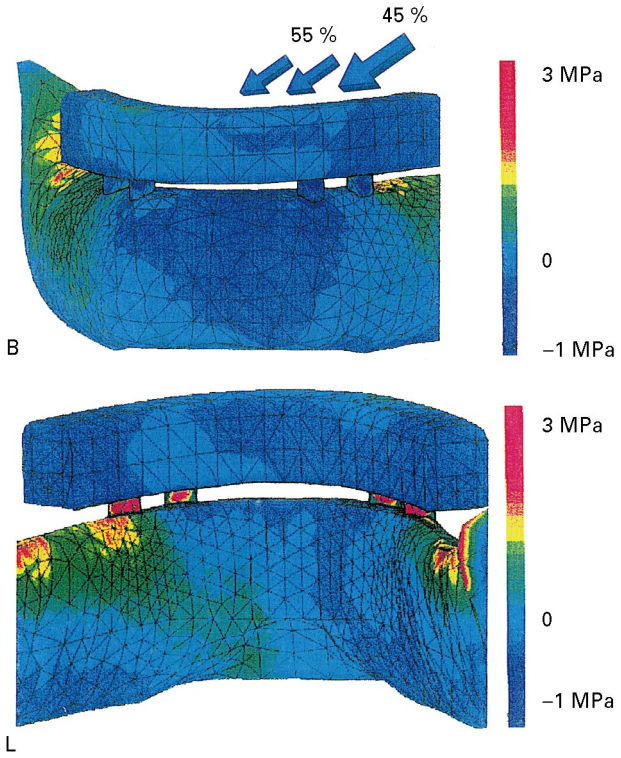

Figure 6 Four-implant model: comparison of the stress distribution in the mandible section at the distal implant site for the posterior (left) and anterior (right) group functions.

4. Conclusions

The different prosthetic architectures do not allow direct comparison between stresses in the distally supported and cantilevered restoration for different occlusal schemes. However, the bone–implant interface is differently loaded by the posterior and anterior group functions.

In the cantilever system, supported by four implants, the posterior group function produces an apical stress concentration at the bone–implant interface, while a more uniform stress distribution along the interface is produced by the anterior group function. This feature is in accordance with the work of Hobo *et al.* [11].

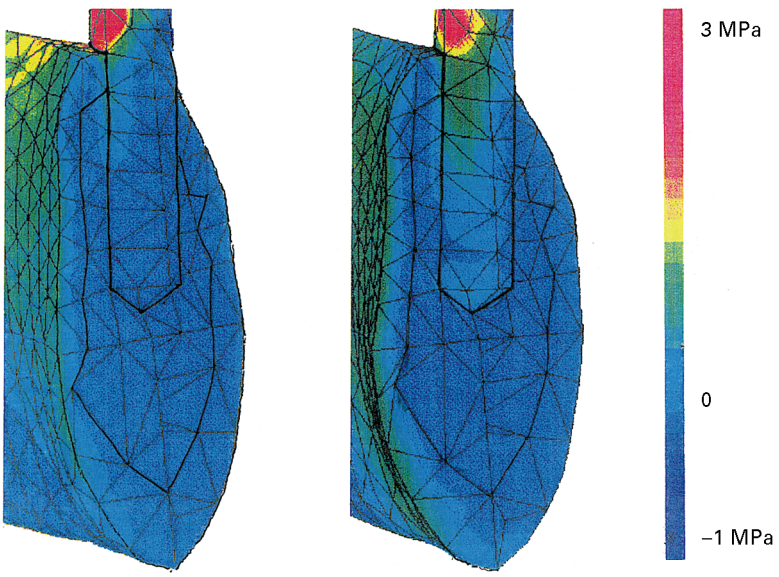

Figure 7 Four-implant model (second occlusal scheme): map of the stress distribution in the anterior group function.

Conversely, the reverse effect is observed in the six-implant system. The highest stress concentration in the aptical zone is induced by the anterior group function, while a more uniform distribution is observed in the posterior group function scheme.

The biomechanical behaviour of the canine guidance is equivalent to the anterior group function.

1. The occlusal scheme in the stress distribution at the bone–implant interface and at the cortical bone is relevant.

2. Within the limits of the FE model simulation, it seems that the more favourable occlusal scheme for the cantilevered implant restorations is the anterior group function, while in distally supported restorations the posterior group function is to be preferred.

3. Further developement of such analysis involves optimization of the selection of implant type in differently located mandibular sites according to each occlusal scheme.

References

1. P. E. DAWSON, "Evaluation, diagnosis and treatment of occlusal problems (C. V. Mosby, St Louis, MO, 1974).
2. J. P. STANDLEE, A. A. CAPUTO and J. P. RALPH, *J. Prosthet. Dent.* **41** (1979) 35.
3. S. P. RAMFJIORD and M. M. ASH, "Occlusion". (W. B. Saunders Philadelphia, PA, 3rd Edn, 1983).
4. A. BAUER, A. GUTOWSKI, "Gnatologia. Introduzione teorica e pratica" (Piccin Nuova Libraria, Padova, 1984).
5. N. D. MOHL, G. A. ZARB, G. E. CARLSSON and J. D. RUGH, "A textbook of occlusion" (Quintessence Publishing, Chicago, IL, 1988).
6. P.-I. BRANEMARK, *J. Prosthet. Dent.* **50** (1983) 39.
7. U. LEKHOLM, *ibid.* **50** (183) 116.
8. J. B. BRUNSKI, *Int. J. Oral Maxillofac. Implants* **3** (1988) 85.
9. P.-I. BRANEMARK, B. O. HANSSON, R. ADELL, U. BREINE, J. LINDSTROM, O. HALLEN and A. OHMAN, "Osseointegrated implants in the treatment of the edentulous jaw. Experience from a 10-year period (Almquist and Wiksell, Stockholm, 1977).
10. T. JEMT, S. LUNDQUIST, B. HEDEGARD, *J. Prosthet. Dent.* **48** (1982) 719.
11. S. HOBO, E. ICHIDA and L. T. GARCIA, "Osseointegration and occlusal rehabilitation" (Quintessence Publishing, Chicago, IL, 1990).
12. B. RANGERT, T. JEMT, L. JPRNEUS, *Int. J. Oral Maxillofac. Implants* **4** (1989) 241.
13. S. HOBO and H. ITOH, *J. Gnathol.* **9** (1990) 49.
14. J. V. REITZ, *Quintessence Int.* **25** (1994) 177.
15. I. P. VAN ROSSEN, L. H. BRAAK, C. de PUTTER and K. de GROOT, *J. Prosthet, Dent.* **64** (1990) 198.
16. Y. MATSUSHITA, M. KITOH, K. MIZUTA, H. IKEDA and T. SUETSUGU, *J. Oral Implantol.* **17** (1990) 6.
17. F. SIMIONATO, "Tecnologie dei materiali dentali", Vol. 1, Part II (Piccin Nuova Libraria, Padova, 3rd Edn, 1985).
18. S. HOBO and Y. H. JO, *J. Gnathol.* **10** (1991) 9.

Received 19 January 1996
and Accepted 28 January 1997